

Electron Energy Loss Spectroscopy of strongly correlated systems in infinite dimensions

Luis Craco¹ and Mukul S.Laad²

¹*Instituto de Fisica “Gleb Wataghin” - UNICAMP, C.P. 6165, 13083-970 Campinas - SP, Brazil*

²*Institut fuer Theoretische Physik, Universitaet zu Koeln, Zuelpicher Strasse, 50937 Koeln, Germany*

(November 13, 2018)

We study the electron-energy loss spectra of strongly correlated electronic systems doped away from half-filling using dynamical mean-field theory ($d = \infty$). The formalism can be used to study the loss spectra in the optical ($\mathbf{q} = \mathbf{0}$) limit, where it is simply related to the optical response, and hence can be computed in an approximation-free way in $d = \infty$. We apply the general formalism to the one-band Hubbard model off $n = 1$, with inclusion of site-diagonal randomness to simulate effects of doping. The interplay between the coherence induced plasmon feature and the incoherence-induced high energy continuum is explained in terms of the evolution in the local spectral density upon hole doping. Inclusion of static disorder is shown to result in qualitative changes in the low-energy features, in particular, to the overdamping of the plasmon feature, resulting in a completely incoherent response. The calculated EELS lineshapes are compared to experimentally observed EELS spectra for the normal state of the high- T_c materials near optimal doping and good qualitative agreement is found.

PACS numbers: 75.30.Mb, 74.80.-g, 71.55.Jv

The ac conductivity and dielectric tensor provides valuable information concerning the finite frequency, finite temperature charge dynamics of an electronic fluid in a metal. The dramatic changes in the electronic state from localized to itinerant across an insulator-metal (I-M) transition, be it driven by pressure, or doping the insulator, is reflected in concomitant changes in the optical responses. These studies, therefore, give one a systematic picture describing the nature of the change in electronic state, appearance of new low-energy excitations, their dispersion and stability. In cuprate superconductors, for e.g, these studies have convincingly demonstrated the non-Fermi liquid nature of the charge [1] and spin [2] dynamics in the normal state.

Optical response in a solid provides an estimate of the carrier scattering rate at finite frequency, and thus give detailed information about the finite frequency collective excitations responsible for scattering the carriers. In a quantum paramagnetic metal, the dominant carrier-scattering mechanism are electron-hole pairs, which are the low-energy collective excitations- it is precisely the e-h spectrum which is measured by electron-energy-loss spectroscopy (EELS), which provides one with a direct experimental picture for the spectral density of particle-hole excitations in a solid [3].

In a weakly interacting system, one expects the details of the particle-hole spectrum to be sensitive to details of the shape and size of the Fermi surface (e.g, its curvature). That such a picture is untenable for strongly correlated systems was pointed out by Shastry *et al* [4], who argued that in this case, the whole Brillouin zone tends to get populated. Another important point of considerable relevance is the transfer of spectral weight over large energy scales that is characteristic of strongly correlated systems-it has no analog in weakly interacting fermi sys-

tems. Consequently, one expects qualitatively different responses in this case, compared to those characteristic of weakly interacting systems.

Quite generally, the transmission EELS lineshape is related to the wave-vector and frequency dependent dielectric function via the equation,

$$I(\mathbf{q}, \omega) = -Im \frac{1}{\epsilon(\mathbf{q}, \omega)}. \quad (1)$$

Following Ref. [3], we employ the random-phase-approximation (RPA) to treat the small- \mathbf{q} part. In the optical limit that we are interested in ($q \rightarrow 0$), $\epsilon(\mathbf{q} \rightarrow 0, \omega) = 1 + 4\pi \frac{i\sigma(\omega)}{\omega}$, where $\sigma(\omega)$ is the longitudinal optical conductivity. The analysis carried out along these lines is invalid when $qa \simeq 1$, where the short-ranged part of the potential has to be considered and the RPA is inadequate. However, local correlation effects are correctly incorporated into the above eqn via $\sigma(\omega)$, which can be computed reliably within $d = \infty$, for example. In this limit, $\mathbf{q} \simeq 0$, the particle-hole spectral density is obtainable from the dissipative part of [3],

$$I(0, \omega) = -Im \frac{1}{\epsilon(0, \omega)} = \frac{\epsilon''(\omega)}{\epsilon'^2(\omega) + \epsilon''^2(\omega)} \quad (2)$$

with $\epsilon'(\omega) = 1 - \frac{4\pi\sigma''(\omega)}{\omega}$ and $\epsilon''(\omega) = \frac{4\pi\sigma'(\omega)}{\omega}$ so that one needs to have an estimate of the longitudinal dielectric constant to calculate the EELS spectrum. It is to be noted that this yields the EELS lineshape corresponding to the experiment performed in the so-called "transmission mode". Thus, the problem has now been reduced to that of computing $\epsilon(\omega)$, which, being a local quantity, can be computed in an approximation-free way in $d = \infty$ [5].

In this communication, we want to develop a theory of the transmission EELS (eq. (1)) for electronic systems

which undergo Mott transitions as a function of band-filling [5]. To be specific, we consider the one-band Hubbard model, where the Mott transition can be driven by hole-doping the Mott insulator, or by pressure (which changes the ratio U/t). To capture more fully the effects of chemical substitution-(which is how doping is carried out in practice), we also introduce static, site-diagonal disorder in the model. The resulting hamiltonian is,

$$H = - \sum_{ij\sigma} t_{ij} c_{i\sigma}^\dagger c_{j\sigma} + U \sum_i n_{i\uparrow} n_{i\downarrow} - \sum_{i,\sigma} (v_i - \mu) n_{i\sigma} \quad (3)$$

as a prototype model describing the electronic degrees of freedom in TM oxides. To study the 3D case, we employ the $d = \infty$ approximation, which is the best among those currently available to study the M-I transition [5]. Since this method has been extensively reviewed, we only summarize the relevant aspects. All transport properties, which follow from the conductivity tensor, are obtained from a \mathbf{k} -independent self-energy in $d = \infty$; the only information about the lattice structure comes from the free band dispersion in the full Green fn:

$$G(k, \omega) = G(\epsilon_k, \omega) = \frac{1}{\omega + \mu - \epsilon_k - \Sigma(\omega)} \quad (4)$$

To solve the model in $d = \infty$ requires a reliable way to solve the single impurity Anderson model(SIAM) embedded in a dynamical bath described by the hybridization fn. $\Delta(\omega)$. There is an additional condition that completes the selfconsistency:

$$\int d\epsilon G(\epsilon, i\omega) \rho_0(\epsilon) = \frac{1}{i\omega + \mu - \Delta(i\omega) - \Sigma(i\omega)} \quad (5)$$

where $\rho_0(\epsilon)$ is the free DOS ($U = 0$). The above eqns. (3-4) refer to the disorder-free Hubbard model. With microscopic, binary disorder (which is the only type we consider here),

$$P(v_i) = (1 - x)\delta(v_i) + x\delta(v_i - v) \quad (6)$$

only the disorder-averaged quantities are physically observable. In this case, we use an extended version of the iterated perturbation theory (IPT), which combines the effects of dynamical correlations (via usual IPT) with those of disorder (via CPA) in a selfconsistent way. For the sake of completeness, we outline the calculational details briefly. As a first step, we compute the full local Green function for the pure model using IPT. This has been shown [5] to yield results in excellent agreement with those obtained from exact diagonalization techniques. This IPT propagator is then corrected for repeated scattering from local disorder by computing the new self energy from the usual CPA [6],

$$\langle T_{ii}[\Sigma(\omega)] \rangle_c = \frac{-(1-x)\Sigma(\omega)}{1 + \Sigma(\omega)G(\omega)} + \frac{x(v - \Sigma(\omega))}{1 - (v - \Sigma(\omega))G(\omega)} = 0 \quad (7)$$

which results in an implicit equation for the interaction and disorder corrected self energy (and Green function). To make the treatment selfconsistent, we compute the new IPT selfenergy using the new GF computed with (IPT+CPA) in the first step. This procedure is repeated until convergence is achieved. At each step of the iteration, we fix the chemical potential from the Luttinger sum rule, $n = \int_{-\infty}^{\mu} \rho(\omega) d\omega = x$. This extended IPT yields the local propagator, $\langle G_{ii}(\omega) \rangle$ corrected both for dynamical correlations and disorder induced repeated scattering, both treated on the same footing [6]. In $d = \infty$, this is sufficient to compute the transport, because the vertex corrections in the Bethe Salpeter eqn. for the conductivity vanish identically in this limit [7]. Thus, the conductivity is fully determined by the basic bubble diagram made up of fully interacting local GFs of the lattice model.

The optical conductivity and the Hall conductivity are computable in terms of the full $d = \infty$ GFs as follows [7]:

$$\sigma_{xx}(i\omega) = \frac{1}{i\omega} \int d\epsilon \rho_0(\epsilon) \sum_{i\nu} G(\epsilon, i\nu) G(\epsilon, i\nu + i\omega) \quad (8)$$

The dynamical dielectric constant is directly calculated from the optical conductivity via,

$$\epsilon_{xx}(\omega) = 1 + \frac{4\pi}{\omega} i\sigma_{xx}(\omega) \quad (9)$$

yielding its real and imaginary parts. Use of eqn.(3) then permits us to study $I_{EELS}(\omega) = -Im \frac{1}{\epsilon(\omega)}$,

Before embarking on our results and their analysis, it is instructive to summarize what is known about the $d = \infty$ Hubbard model. At large U/t , and away from half-filling ($n = 1$), the ground state is a paramagnetic FL if one ignores the possibility of symmetry breaking towards antiferromagnetism, as well as disorder effects, which are especially important near $n = 1$. This can be achieved formally by introducing a nnn hopping, which in $d = \infty$ leaves the free DOS essentially unchanged [5]. This metallic state is characterized by two energy scales: a low energy coherence scale T_{coh} , below which local FL behavior sets in [5], and a scale of $O(D)$, (D is the free bandwidth) characterizing high energy, incoherent processes across the remnant of the Mott-Hubbard insulator at $n = 1$. At $T < T_{coh}$, the quenching of the local moments leads to a response characteristic of a FL at small $\omega \ll 2D$ (but with the dynamical spectral weight transfer with doping, a feature of correlations), but at higher $T > T_{coh}$, the picture is that of carriers scattered off by effectively local moments, which makes the system essentially like a non-FL (note that the metal with disordered local moments is not a FL).

The picture is modified drastically in presence of static, diagonal disorder, in which case, the extended IPT has to be used. For weak disorder, the above picture is qualitatively unaffected, and the only interesting features are

that Luttinger's theorem is violated, and the FL quasiparticles acquire a finite lifetime at μ [6]. However, with increasing disorder, repeated scattering effects destroy the quasiparticle picture, and the metallic state is characterized by an incoherent, non-FL response with a pseudogap structure in the DOS. Similar results have been obtained earlier in Ref. [8], where a T -matrix approximation was employed to treat disorder-induced resonant scattering. The above describes the competing tendency of the correlation-induced low temperature coherence scale, T_{coh} in the $d = \infty$ Hubbard model, with the disorder-induced incoherence, which tends to suppress it, driving it eventually to zero, leading to a non-FL metal state. A large enough disorder strength leads to band-splitting, as in usual CPA, leading to a continuous transition to a disorder driven insulating state.

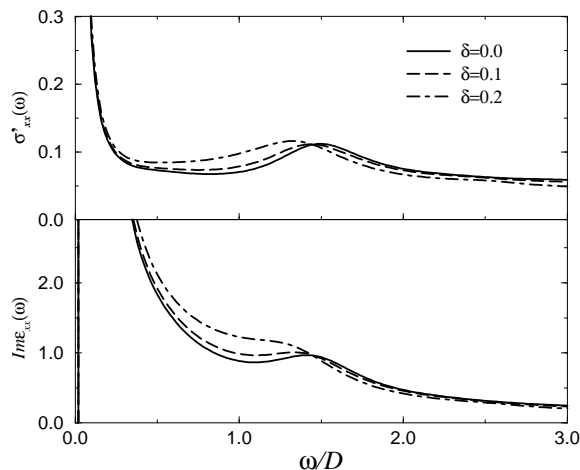


FIG. 1. Real part of the optical conductivity σ_{xx} for $U/D = 3.0$, $\delta = 0.1$ (continuous) and $\delta = 0.2$ (dot-dashed). The lower panel shows the imaginary dielectric constant for the same parameter values. Note the isosbestic point in both quantities.

Armed with this information, we are ready to discuss our results. We choose a gaussian unperturbed DOS, and $U/D = 3.0$ to access the strongly correlated FL metallic state off $n = 1$, ignoring the possible instability to an AF-ordered phase. All calculations are performed at a low temperature, $T = 0.01D$. We are mainly interested in the variation of the EELS lineshape with hole doping, given here by $\delta = (1 - n)$. This fixes the chemical potential, and the FL resonance position, and the IPT describes the evolution of spectral features in good agreement with exact diagonalization studies [5]. In view of the ability of the IPT to reproduce all the qualitative aspects observed in $\sigma_{xx}(\omega)$, we believe that is a good tool in the present case. Fig.(1) shows the optical conductivity and the longitudinal dielectric constant. $\sigma_{xx}(\omega)$ agrees with calculations performed earlier in all the main

respects; in particular, it clearly exhibits the low-energy quasicohherent Drude form, the transfer of optical spectral weight from the high-energy, upper-Hubbard band states to the low energy, band-like states with increasing hole doping, and the isosbestic point at which *all* the $\sigma_{xx}(\omega)$ curves as a fn. of filling cross at one point, to within numerical accuracy. It is interesting to point out that such features have also been observed in experimental studies [10]. Correspondingly, $\text{Im}\epsilon_{xx}(\omega)$ also shows the isosbestic point, the explanation for which is identical to the heuristic one proposed recently by us for the case of $\sigma_{xx}(\omega)$ [11].

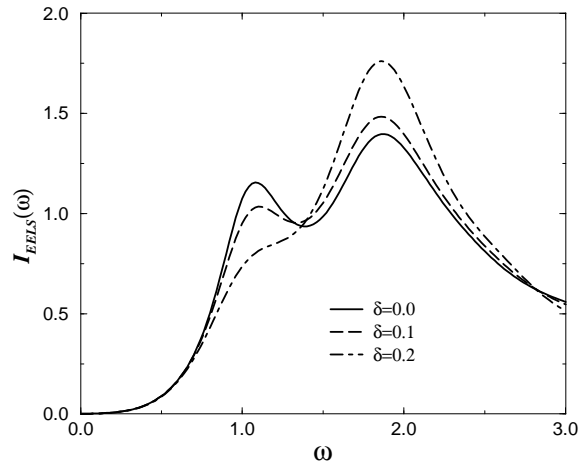


FIG. 2. The electron-energy loss spectra for the doped Hubbard model for $U/D = 3.0$, and $\delta = 0.1, 0.2, 0.3$ as shown. The curve with circles denotes the Drude contribution from renormalized single-hole excitations in the metallic phase.

In Figs. 2 and 3, we show the theoretically calculated EELS spectrum for $U/D = 3.0$ and for different band-fillings as a function of disorder strength, v . This allows us to access the intermediate correlation regime, where the absence of any small parameter in the problem requires use of controlled methods that interpolate correctly between the weak- and strong coupling limits (such as the $d = \infty$ method used here). From the calculation of the optical response, we have checked that $\text{Im}\sigma_{xx}(\omega = 0) = 0$, implying that $-Re1/\epsilon(0) = 0$, as required [12]. With $U/D = 3.0$, we observe a peak at $\omega \simeq U/2$, associated with the transitions from the lower-Hubbard band to the quasiparticle resonance. We associate this peak to the strongly renormalized particle-hole excitations in the strongly correlated metal. In this context, two features are worthy of mention: at low energy, the loss intensity goes quadratically with ω , and the particle-hole peak position shifts with increasing doping. The shift of this feature correlates with that of the mid-IR peak in the optical conductivity (Fig.(1)), and is thus a clear manifestation of the transfer of optical weight

to lower energy with hole-doping. Moreover, appreciable loss intensity is observed at higher energies ($\omega > 2.0$) as a smooth continuum, in contrast to the expectations from a weakly correlated (very small U/D) FL. This clearly shows how the delicate balance between coherence and incoherence is controlled by the transfer of optical spectral weight in the full EELS spectrum. In fact, we expect the coherent feature in the full spectrum to become sharper as T ($0.01D$ in our analysis) is lowered further. We see from the above that coupling to high-energy, incoherent, multiparticle excitations strongly renormalizes, but does not destroy, the coherent response in a strongly correlated Fermi liquid. However, the analysis presented above shows that a proper treatment of coherence (related to itinerance) and incoherence (coming from the local, atomic-like features) on an equal footing is necessary to obtain consistent results. The EELS at very low energy are well described by a Drude fit, but features like the damped plasmon peak at $\omega/D \simeq 1.0$ are distinctly non-Drude-like, and can only be reliably accessed by the full analysis, as described above.

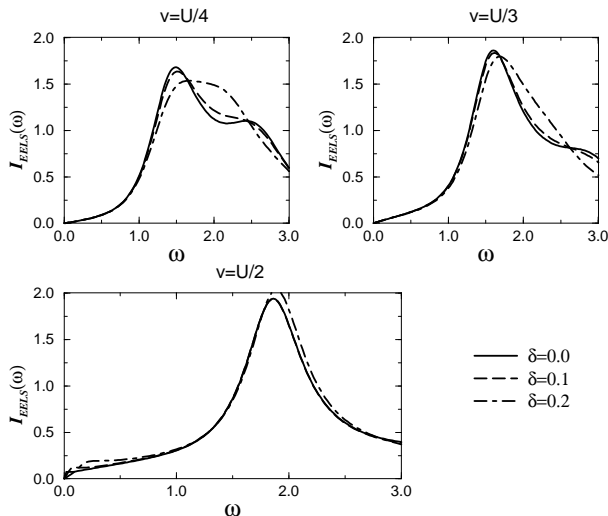


FIG. 3. The EELS spectra for the $d = \infty$ Hubbard model for $U/D = 3.0$ and $v/U = 1/4, 1/3, 1/2$. See the text for the explanation of various structures in $I_{EELS}(\omega)$ in the light of the underlying structure of the local spectral density of the HM in $d = \infty$.

Given the above, we expect small coherence destroying perturbations to tilt the balance in favor of low-energy incoherence. Consideration of doping-induced static disorder has precisely such an effect on the low energy EELS spectrum. Consistent with the disorder-induced smearing of the Drude part in $\sigma_{xx}(\omega)$, the coherent part in the EELS spectrum is replaced by a broad peak, which still shows remnants of the coherent peak at $v = 0$ ($v = U/4$). However, the low-energy ω^2 dependence in the pure case is replaced by a *linear* ω dependence in this case. The complete destruction of the quasiparticle behavior in the

DOS and the Drude-like response at $v = U/3$ is consistent with the complete destruction of the “coherent” peak in the EELS spectrum; we understand this as overdamping of the collective p-h peak by disorder-induced strong scattering as v is increased. In the strong disorder regime, the metallic state is incoherent with a pseudogap feature in the DOS [11], and the action of the potential $V_{\mathbf{k}\mathbf{k}'}$ between the Hubbard band states does not create well-defined elementary excitations, leading to an incoherent response at low energy.

In experiments carried out on the cuprates in their normal state, a very broad plasmon peak is revealed [12], implying poorly defined plasmon excitations in the correlated metallic state. These studies also reveal that the optic “plasmon” disperses quadratically (in q). Recent studies indicate an acoustic-like heavily damped plasmon mode at small \mathbf{q} [13] with a *linear* ω dependence in $Bi_2Sr_2CaCu_2O_8$, alongwith a single broad peak. We cannot directly compare our results to those of [13], the EELS experiment was carried out in the reflection mode, and this measures the quantity $Img(0, \omega)$, which is not directly related to what we have calculated here. However, looking at the results of [12], we see that the essential features seen there are indeed reproduced by our calculation. To make contact between our calculations and experiments, we shall suppose that the one-band Hubbard model is understood to be the *effective* model describing the coupled spin-carrier dynamics in the Cu-O planes. We will also assume that bandstructure effects are not crucial to the case under study, and that the source of the anomalous behaviors is rooted in the dynamical effects of the strong, local Hubbard interaction, an assumption well-supported at doping levels near the optimal [14]. We stress that the above conditions will be modified in the pseudogap phase, where the precursor effects of *d*-wave pairing fluctuations-intrinsically non-local, are appreciable [15]. In this doping range, the dynamical effects of non-local correlations will probably lead to even stronger deviations from a FL picture, though a concrete calculation including such effects remains to be developed. With these caveats in mind, we find good qualitative agreement between our results for $v = U/3$ of Fig. 3 and the experimental EELS lineshapes [12]; the quadratic (in ω) behavior at low ω , the broad “plasmon” peak (strongly damped), the asymmetric lineshape and the continuum response at higher energy are all reproduced in qualitative agreement with experiment. It would be interesting to check whether the plasmon peak shifts to lower energies with hole doping; this would be an interesting check on the validity of the approach presented here. The comparison is quite good upto $\omega/D \simeq 3.0$, beyond which the simple single-band modelling does not apply anyway.

There is extensive experimental work [16] indicating that the metallic phase above T_c near optimal doping in cuprates is not describable in terms of Landau Fermi liq-

uid ideas. Prelovsek *et al.* [17] have recently considered the question of the EELS lineshape in the $t - J$ model, making use of results obtained from finite-temperature Lanczos techniques. Within our approach, it is known that the metallic state off $n = 1$ above the lattice coherence scale, T_{coh} , is not a Fermi liquid [5]; the calculation carried out above is then consistent with the non-FL charge dynamics if the T_{coh} can be driven sufficiently low (below $0.01D$ used here). We expect precisely a very low T_{coh} near $n = 1$ for U/D near the Mott transition [5]. Comparing our results with those found in [17], we observe that our results are in nice agreement with theirs, but the results presented here are more transparent, being based on an analytical scheme. In addition, the results show that the $d = \infty$ approach is capable of producing the low- and high-energy features on the same footing, and moreover, permits us to include effects of doping-induced static disorder in a consistent way. In view of this, we believe that the approach described here should also be applicable to a wide variety of doped transition metal oxides, where the combined effects of correlations and disorder are especially pronounced [2]. Additionally, effects of orbital degeneracy, etc, in real materials can be treated by a suitable generalization of the above procedure [5]. This is a non-trivial problem, because the solution of the impurity model is harder. We hope to address this issue in future work.

In conclusion, we have considered the energy loss function of a model for transition metal oxides, and captured the effects of strong, local correlations and static disorder in a consistent way. Comparison of our results with the experimental EELS spectra for cuprates in the “normal” state above T_c near optimal doping shows that all the main observed features are consistently reproduced by our calculation.

ACKNOWLEDGMENTS

LC was supported by the Fundação de Amparo à Pesquisa do Estado de São Paulo (FAPESP). MSL thanks Prof. E. Müller-Hartmann for encouragement and advice and Prof. G. Sawatzky for a discussion of the experimental results. MSL was supported by the Sfb 341 of the DPG.

- [4] For a good theoretical review of the Hall effect in strongly correlated systems, see B. S. Shastry *et al.*, Phys. Rev. Lett. **70**, 2004 (1993); **71**, 2838 (1993).
- [5] A. Georges *et al.* Revs. Mod. Phys. **68**, 13 (1996).
- [6] V. Dobrosavljevic *et al.* Phys. Rev. Lett. **69**, 1113 (1992), E. Miranda *et al.* Phys. Rev. Lett. **78**, 290 (1997), M. S. Laad *et al.* submitted to Phys. Rev. B (cond-mat 9911378).
- [7] A. Khurana, Phys. Rev. Lett. **64**, 1990 (1990).
- [8] D. Cox, in “Proceedings of the Workshop on Non-Fermi Liquids”, J. Phys: Condens. Matter **8** (1996).
- [9] For a review of the different techniques used to solve the impurity problem in the large- d context, see A. Georges *et al.* Revs. Mod. Phys. **68**, 13 (1996).
- [10] See for example, the various cases discussed in the review of Ref. [2].
- [11] M. S. Laad *et al.*, cond-mat 9907328.
- [12] See, for e.g, I. Bozovic, Phys. Rev. B **42**, 1969 (1990). see also, N. Nücker *et al.*, Phys. Rev. B **39**, 12379 (1989).
- [13] K. Schulte *et al.*, unpublished. I thank G. Sawatzky for a discussion of the EELS lineshapes in the normal, near optimal doped $Bi_2Sr_2CaCu_2O_8$ superconductor.
- [14] This fact underlies the success of the marginal Fermi liquid phenomenology in understanding many aspects of normal state data of cuprates near optimal doping. The approach is characterized by a predominantly local, anomalous collective susceptibility and self-energy, justifying the use of the $d = \infty$ approximation used here; see for e.g, C. M. Varma *et al.* Phys. Rev. Lett. **63**, 1996 (1989).
- [15] The dynamical effects of d -wave pair fluctuations, shown to be important in the pseudogap phase in the underdoped region of the phase diagram of cuprates (M. Randeria, Varenna Lectures, cond-mat 9711232), are intrinsically non-local, and hence are out of the scope of the $d = \infty$ based theories.
- [16] A vast literature exists, but a complete picture for the breakdown of Fermi liquid ideas in the normal state of cuprates is by P. W. Anderson, in “The Theory of High- T_c Superconductivity in Cuprates”, Princeton University Press (1997).
- [17] P. Prelovsek *et al.* Phys. Rev. B **60**, R3735 (1999).

-
- [1] D. B. Tanner *et al.*, in “Physical Properties of High Temperature Superconductors III”, ed. D. M. Ginsberg (World Scientific, Singapore, 1992), p. 363.
 - [2] M. Imada *et al.* Revs. Mod. Phys. **70**, 1039, (1999).
 - [3] D. Pines and P. Nozieres, “The Theory of Quantum Liquids”, (Benjamin, NY, 1966, Vol.1).